# Surface-Enhanced Raman Spectroscopy of Soft-Landed Polyatomic Ions and Molecules

**Michael Volný,[†] Atanu Sengupta,[‡] C. Brant Wilson,[‡] Brian D. Swanson,[§] E. James Davis,[‡] and František Tureček*,[†]**

*Departments of Chemistry, Chemical Engineering, and Earth and Space Sciences, University of Washington, Seattle, Washington 98195-1700*

**Surface-enhanced Raman spectroscopy (SERS) was used to detect and characterize polyatomic cations and molecules that were electrosprayed into the gas phase and soft-landed in vacuum on plasma-treated silver substrates. Organic dyes such as crystal violet and Rhodamine B, the nucleobase cytosine, and nucleosides cytidine and 2′-deoxycytidine were immobilized by soft landing on plasma-treated metal surfaces at kinetic energies ranging from near thermal to 200 eV. While enhancing Raman scattering $10^5-10^6$-fold, the metal surface effectively quenches the fluorescence that does not interfere with the Raman spectra. SERS spectra from submonolayer amounts of soft-landed compounds were sufficiently intense and reproducible to allow identification of Raman active vibrational modes for structure assignment. Soft-landed species appear to be microsolvated on the surface and bound via ion pairing or $\pi$-complexation to the Ag atoms and ions in the surface oxide layer. Comparison of spectra from soft-landed and solution samples indicates that the molecules survive soft landing without significant chemical damage even when they strike the surface at hyperthermal collision energies.**

Interactions of hyperthermal ions with surfaces have been of both fundamental and practical interest in processes such as ion sputtering, dissociation, implantation, and epitaxy.[1] A particular application of collisions with surfaces of hyperthermal ions having kinetic energies in the range of 5−100 eV is referred to as "soft landing" in which the species striking the surface are not sputtered off but remain deposited on the surface.[2] Of the many applications of soft landing, those concerning biomolecules, such as amino acids and peptides,[3] DNA fragments,[4] and even intact viral particles,[5] have been of much recent interest. It has been shown that gas-phase ions produced from organic molecules[6] as well as large biopolymers, such as proteins and polysaccharides, can be nondestructively landed from vacuum onto solid surfaces[7,8] or into liquid matrixes[9] and recovered with retention of biological activity. The biomolecules are typically injected into the gas phase by electrospray, a nondestructive ionization method[10] that produces multiply protonated or sodiated cations, or deprotonated anions. These are transferred to the vacuum system at preparatively relevant fluxes as high as 750 pmol/h.[11] Soft landing has opened new avenues for various applications, such as surface modifications,[2a,b] fabrication of protein arrays,[12] bioactive metal surfaces for medical implants,[7,13] and multiplex separations using the mass spectrometer as a preparative device for biomolecules.[14] For multiply charged ions, the properties of the soft-landed material appear not to depend on the charge state.[9] Previous results have shown that mass analysis prior to soft landing, albeit desirable,[14] is not critical in soft-landing experiments.[11] In addition to ion soft landing, recent studies have also revealed that colliding multiply charged ions with oxide-coated metal surfaces at slightly elevated kinetic energies, typically in the range of 40−200 eV, resulted in nondestructive discharge and immobilization of the biomolecules

* To whom correspondence should be addressed. E-mail: turecek@chem.washington.edu.

† Department of Chemistry.

‡ Department of Chemical Engineering.

§ Department of Earth and Space Sciences.

(1) Rabalais, J. W., Ed. *Low Energy Ion−Surface Interactions*; Wiley: Chichester, 1994.

(2) (a) Franchetti, V.; Solka, B. H.; Baitinger, W. R.; Amy, J. W.; Cooks, R. G. *Int. J. Mass Spectrom. Ion Phys.* **1977**, *23*, 29−35. (b) Grill, V.; Shen, J.; Evans, C.; Cooks, R. G. *Rev. Sci. Instrum.* **2001**, *72*, 3149−3179. (c) Hanley, L.; Sinnott, S. B. *Surface Sci.* **2002**, *500*, 500−522. (d) Cooks, R. G.; Jo, S. C.; Green, J. *Appl. Surf. Sci.* **2004**, *231*, 13−21.

(3) (a) Nanita, S. C.; Takacz, Z.; Cooks, R. G. *J. Am. Soc. Mass Spectrom.* **2004**, *15*, 1360−1365. (b) Alvarez, J.; Cooks, R. G.; Barlow, S. E.; Gaspar, D. J.; Futrell, J. H.; Laskin, J. *Anal. Chem.* **2005**, *77*, 3452−3460. (c) Gologan, B.; Green, J. R.; Alvarez, J.; Laskin, J.; Cooks, R. G. *Phys. Chem. Chem. Phys.* **2005**, *7*, 1490−1500.

(4) Feng, B.; Wunschel, S. S.; Masselon, C. D.; Pasa-Tolic, L.; Smith, R. D. *J. Am. Chem. Soc.* **1999**, *121*, 8961−8962.

(5) Siuzdak, G.; Bothner, B.; Yeager, M.; Brugidou, C.; Fauquet, C. M.; Hoey, K.; Chang, C. M. *Chem. Biol.* **1996**, *3*, 45−48.

(6) Geiger, R. J.; Melnyk, M. C.; Busch, K. L.; Barlett, M. G. *Int. J. Mass Spectrom.* **1999**, *182/183*, 415−422.

(7) Kitching, K. J.; Lee, H.-N.; Elam, W. T.; Tureček, F.; Ratner, B. D.; Johnston, E. E.; MacGregor, H.; Miller, R. J. *Rev. Sci. Instrum.* **2003**, *74*, 4832−4839.

(8) Volný, M.; Elam, W. T.; Ratner, B. D.; Tureček, F. *Anal. Chem.* **2005**, **77**, 4846−4853.

(9) (a) Ouyang, Z.; Takats, Z.;. Blake, T. A ; Gologan, B.; Guymon, A. J. ; Wiseman, J. M.; Oliver, J. C.; Davisson, V. J.; Cooks, R. G. *Science* **2003**, *301*, 1351−1354. (b) Gologan, B.; Takacz, Z.; Alvarez, J.; Wiseman, J. M; Talaty, N.; Ouyang, Z.; Cooks, R. *J. Am. Soc. Mass Spectrom.* **2004**, *15*, 1874−1884.

(10) (a) Yamashita, M.; Fenn, J. B. *J. Phys. Chem.* **1984**, *88*, 4451−4459. (b) Morozov, V. N.; Morozova, T. Ya. *Anal. Chem.* **1999**, *71*, 3110−3117.

(11) Volný, M.; Tureček, F. *J. Mass Spectrom.* **2006**, *41*, 124−126.

(12) Blake, J. B.; Ouyang, Z.; Wiseman, J. M.; Takats, Z.; Guymon, A. J.; Kothari, S.; Cooks, R. G. *Anal. Chem.* **2004**, *76*, 6293−6305.

(13) Volný, M.; Elam, W. T.; Ratner, B. D.; Tureček, F. *J. Biomed. Mater. Res., B: Appl. Biomater.* **2006**, *80B*, 505−510.

(14) (a) Mayer, P. S.; Tureček, F.; Lee, H.-N.; Scheidemann, A. A.; Olney, T. N.; Schumacher, F.; Štrop, P.; Smrčina, M.; Pátek, M.; Schirlin, D. *Anal. Chem.* **2005**, *77*, 4378−4384. (b) Yang, X.; Mayer, P. S.; Tureček, F. *J. Mass Spectrom.* **2006**, *41*, 256−262.

10.1021/ac070278a CCC: $37.00 
Published on Web 05/16/2007

on the surface while retaining their biological functions such as antithrombogenicity,[7,13] enzymatic activity,[8,15] and bioaffinity.[8,15]

The phenomena associated with soft landing of gas-phase ions on oxide-coated metal surfaces have been studied using bioassays and fluorescence spectroscopy.[8,15] While these methods provide valuable information on the biological activity of the surface-tethered material and the presence of intact fluorophores, they lack chemical specificity. In particular, the nature of bonding to the surface and chemical changes in the immobilized molecules are not revealed on a molecular level. Atomic force microscopy (AFM) has been used to visualize soft-landed protein on oxidized metal surfaces,[15] but in general, AFM did not achieve sufficient spatial resolution to recognize fine structural details. X-ray photoelectron spectroscopy (XPS) and secondary ion mass spectrometry have also been used to provide the elemental composition or mass of soft-landed species or their fragments.[16] Previous work also indicated that soft-landed small atomic clusters[17] can be analyzed by using surface-enhanced Raman scattering (SERS).[18,19] SERS provides information on Raman active vibrational modes in molecules that are in a close contact with electrochemically roughened or chemically etched metal surfaces,[20] vapor-deposited metal films,[21] or colloid particles of silver, gold, or platinum[22] and can achieve an amplification of the Raman effect, which is typically on the order of $10^6-10^8$-fold.

We have found that soft landing of polyatomic cations on plasma-treated silver substrates produces samples that reproducibly provide high-quality Raman spectra. The spectra can be used to analyze the Raman active vibrational modes and thus to characterize the surface-bound molecules at detection limits corresponding to submonolayer coverage. In this work, we report the first studies aimed at the detection and structure characterization of soft-landed and immobilized polyatomic cations including organic dyes and nucleosides.

## EXPERIMENTAL SECTION

**Materials.** Chemicals (crystal violet (CV), Rhodamine B, cytosine, cytidine, 2′-deoxycytidine) were purchased from Sigma-Aldrich and used as received. Solvents were purchased from Fisher and were of HPLC grade or certified purity. Silver foil (Sigma-Aldrich, 99.9%, thickness 0.1 mm,) was cut into approximately 15 × 15 mm chips. Prior to plasma treatment, the chips were washed thoroughly with water/methanol/propanol, sonicated in hexane, rinsed with methanol, and allowed to dry.

**Methods. (1) Soft Landing.** Ion soft landing was performed in a vacuum instrument coupled to an in situ plasma reactor as described previously.[7] Briefly, ions were produced by electrospray at atmospheric pressure and transferred to the vacuum system by a heated, glass-lined capillary of 0.8-mm i.d. that was mainteained at 120−150 °C. The gas-phase ions were transported through an intermediate pressure region (0.3−1 Torr) by an electrodynamic ion funnel lens[23] where they undergo 1580−5270 collisions with the residual gas at the indicated pressure. The ions are allowed to pass through a 2-mm aperture to the low-pressure region ($1.4 \times 10^{-3}$ Torr). Ions passing into the second vacuum chamber were focused and transmitted by an rf octopole ion guide maintained at ground potential. We note that the ion guides did not provide mass separation, and thus, all ions of the same polarity with $m/z$ ratios above the mass cutoff of the funnel lens[23b] were transmitted and accelerated to land on the target. The ion beam exiting from the octopole was intercepted by a metal target that was biased by a negative potential providing acceleration for the gas-phase cations to reach kinetic energies in the range of 0−250 eV. The landing target was mounted on a 1-m-long linear motion manipulator that was inserted through a vacuum port in the plasma chamber and extended through a gate valve separating the plasma chamber from the ion optics vacuum chamber. The metallic target was first cleaned and activated by rf discharge plasma operated at 13.56 MHz. After the plasma treatment was finished, the chamber was pumped down and the sample was translated to within 2 mm of the downbeam end of the octopole ion guide where it was exposed to collisions with hyperthermal ions.

The plasma treatment was carried out under a constant flow of $Ar/O_2$ at a constant pressure of 0.25 Torr and 60 W for 15 min. The development of silver oxide was visible by the formation of a dull gray layer on the glossy metallic silver substrate. Most analytes were electrosprayed as methanol/water solutions at 30−300 $\mu$M concentrations in a positive mode under optimized conditions. The ion currents, as measured on the silver target, were typically 1−3 nA. The ions were deposited for 4 h to obtain 100−500 pmol of soft-landed material. Unless stated otherwise, the nominal landing energy for singly charged cations was 40−50 eV as determined by applying a −40 to −50 V potential on the landing plate.

**(2) Confocal Raman Microscopy.** After thoroughly rinsing with methanol and water, the soft-landed samples were placed in an enclosed confocal microscope sample chamber and illuminated with the 514.5-nm line from an Ar ion laser (Coherent Innova 300) that was focused to a 0.8-$\mu m^2$ spot. The scattered light from the sample was collected by the objective lens, redirected, by a series of optical elements, through the confocal microscope pinhole, and focused on the slit of a single-pass Acton SpectraPro-500i monochromator. A Kaiser Optical Systems Supernotch-Plus holographic filter was placed in front of the spectrometer to remove the laser line. The spectrum was recorded using a Princeton Instruments, back-iluminated, liquid nitrogen-cooled 1340 × 1000 pixel array charge-coupled device camera. The laser beam power was typically between 100 and 250 mW, and the exposure time was 60, 300, or 600 s. The spectra were smoothed by adjacent-averaging algorithm with 13 points considered for smoothing. The spectra of soft-landed material were reproduced several times on a commercial


(15) Volný, M.; Elam, W. T.; Branca, A.; Ratner, B. D.; Tureček, F. *Anal. Chem.* **2005**, **77**, 4890−4896.
(16) Alvarez, J.; Futrell, J. H.; Laskin, J. *J. Phys. Chem. A* **2006**, *110*, 1678−1687.
(17) (a) Honea, E. C.; Ogura, A.; Murria, C. A.; Raghavachari, K.; Sprenger, W. O.; Jarrold, M. F.; Brown, W. L. *Nature* **1993**, *366*, 42−44. (b) Haslett, T. L.; Fedrigo, S.; Moskovits, M. *J. Chem. Phys.* **1995**, *103*, 7815−7819.
(18) Fleischmann, M.; Hendra, P. J.; McQuillian, A. J. *Chem. Phys. Lett.* **1974**, *26*, 163−166.
(19) Jeanmaire, D. L.; Van Dyune, R. P. *J. Electroanal. Chem.* **1977**, *84*, 1−20.
(20) Dick, L. A.; McFarland, A. D.; Haynes, C. L.; Van Duyne, R. P. *J. Phys. Chem. B* **2002**, *106*, 853−860.
(21) (a) Davies, J. P.; Pachuta, S. J.; Cooks, R. G.; Weaver, M. J. *Anal. Chem.* **1986**, *58*, 1290−1294. (b) Büchel, D.; Mihalcea, C.; Fukaya, T.; Atoda, N.; Tominaga, J.; Kikukawa, T.; Fuji, H. *Appl. Phys. Lett.* **2001**, *79*, 620−622.
(22) Krug, J. T.; Wang, G. D.; Emory, S. R.; Nie, S. *J. Am. Chem. Soc.* **1999**, *121*, 9208−9214.
(23) (a) Shaffer, S. A.; Tang, K.; Anderson, G. A.; Prior, D. C.; Udseth, H. R.; Smith, R. D. *Rapid Commun. Mass Spectrom.* **1997**, *11*, 1813−1817. (b) Seymour, J. L.; Syrstad, E. A.; Langley, C. C.; Tureček, F. *Int. J. Mass Spectrom.* **2003**, *228*, 687−702.

Renishaw inVia Raman microscope using 514-nm laser excitation and a monochromator grating density of 1200 lines/mm. The wavenumber scale was calibrated with the Raman band of a reference Si(111) surface at 520 $cm^{-1}$. The Raman band wavenumbers were reproducible within 2−3 $cm^{-1}$ absolute deviation between the two instruments and also for measurements of soft-landed samples prepared in the course of several months.

**(3) Mass Spectrometry.** Electrospray mass spectra (ESI-MS) were recorded using a Bruker Esquire quadrupole ion trap instrument equipped with an orthogonal electrospray interface. The ESI-MS spectra were used to confirm the charge state of the ions used in soft landing and to characterize the soft-landed species.

**(4) Atomic Force Microscopy.** AFM measurements were taken in air at room temperature in a tapping mode using a Digital Instruments (Santa Barbara, CA) Digital Multimode IIIa with the standard single silicon crystal cantilever. The data were analyzed by the Digital Nanoscope software version 5.12r3 for Windows NT from the same company.

**(5) X-ray Photoelectron Spectroscopy.** XPS spectra were taken on a Surface Science Instruments S-Probe ESCA instrument. This instrument uses a monochromatized Al Kα X-ray source for photoemission stimulation and a low-energy electron flood gun for charge neutralization. The Service Physics ESCAVB Graphics Viewer program was used to determine peak areas.

**Calculations.** Standard ab initio and density functional theory calculations were performed using the Gaussian 03 suite of programs.[24] Structures were fully optimized with density functional theory calculations using the B3LYP functional[25] and the 6-31+G-(d,p) basis set and characterized as local minima by harmonic frequency calculations including Raman intensities. Optimized geometries and Raman spectra of aqueous molecules and ions were calculated using the refined Polarizable Continuum Model[26] and B3LYP/6-31+G(d,p). Improved energies were obtained by single-point B3LYP and Møller−Plesset (frozen core) calculations with the 6-311+G(2d,p) basis set. The B3LYP and MP2 energies were averaged in the B3-MP2 scheme[27] and used to provide improved relative energies. The calculated energies, enthalpies, entropies, and solvation free energies are given in Table S1 (Supporting Information).

## RESULTS AND DISCUSSION

**Soft Landing and Raman Spectra of Organic Dyes.** Upon electrospray, crystal violet produces singly charged $C_{25}H_{30}N_3$ cations at $m/z$ 372 ($CV^+$). Previous experiments have shown that $CV^+$ survived soft landing on plasma-treated stainless steel and copper surfaces and could be reconstituted and characterized by spectroscopy in solution.[8,11,14] Soft landing of $CV^+$ on plasma-treated silver substrates, followed by spectroscopic analysis of the surface-bound material, produced the Raman spectrum shown in Figure 1. The spectrum obtained from landing $CV^+$ with no potential applied to the target (Figure 1a) shows several intense Raman bands. Most of these bands are also present in the reference spectrum obtained for a 4 mM solution of $CV^+$ chloride in methanol (Figure S1, Supporting Information) and also in the SERS spectrum reported previously for $CV^+$ deposited from aqueous solution on Ag island films.[28] Remarkably, very similar Raman spectra were obtained for $CV^+$ ions that were landed at higher nominal impact energies of 10, 50, and 250 eV (Figures S2−S4, Supporting Information). The Raman spectra showed only minor changes in intensity or band positions when the samples were exposed to multiple washings with methanol each lasting for up to 5 h and repeatedly exposed to the 514-nm excitation line. No photolytic bleaching of the surface-immobilized material was observed under the experimental conditions.

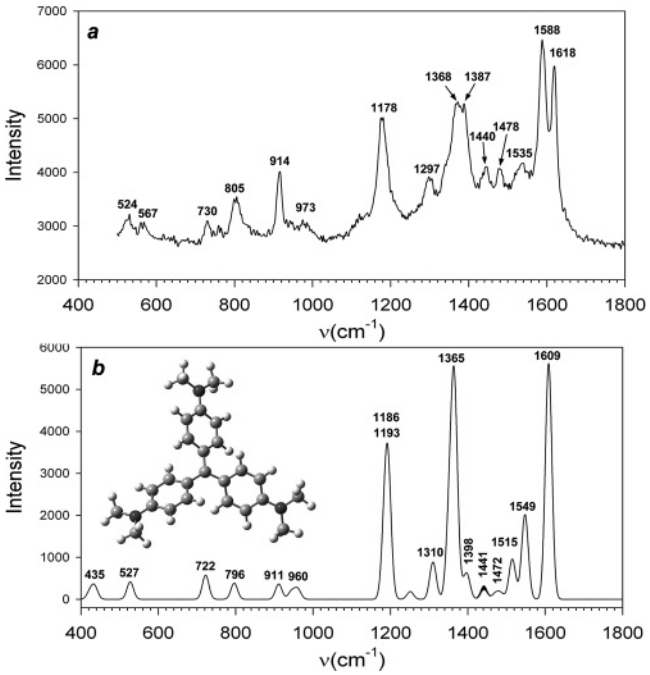


**Figure 1.** (a) SERS spectrum of soft-landed crystal violet cation on a plasma-treated Ag substrate. (b) PCM-B3LYP/6-31G(d) calculated Raman spectrum of $CV^+$ in water. The wavenumbers in the calculated spectrum were scaled by 0.981 and the lines were fitted with Gaussian band shapes at 17 $cm^{-1}$ full width at half-maximum. The inset in Figure 1b shows the optimized structure of $CV^+$.

Multiple blank and control samples were investigated to confirm the identity of the SERS-active species. The Raman spectra of plasma-treated Ag surfaces showed no spectroscopic features. Furthermore, exposing the plasma-treated silver surface to a 3 μM solution of $CV^+$ chloride for up to 15 h, followed by rinsing with solvent, produced no SERS signal from the surface (Figure S5, Supporting Information). Other controls included dipping the plasma-treated Ag substrate into more concentrated $CV^+$ solutions for shorter periods of time or drying 2 nmol of $CV^+$ on the surface (Figure S6, Supporting Information). None of these controls provided a SERS signal of $CV^+$. In contrast, extended washing with methanol of soft-landed $CV^+$ samples caused no significant decrease of or changes in the SERS spectra (Figure S2, Supporting Information). Thus, we conclude that the SERS spectra must

(24) Frisch, M. J.; et al. *Gaussian 03, Revision B.05*; Gaussian, Inc.; Pittsburgh, PA, 2003.
(25) (a) Becke, A. D. *J. Chem. Phys.* **1993**, *98*, 1372−1377. (b) Becke, A. D. *J. Chem. Phys.* **1993**, *98*, 5648−5652. (c) Stephens, P. J.; Devlin, F. J.; Chabalowski, C. F.; Frisch, M. J. *J. Phys. Chem.* **1994**, *98*, 11623−11627.
(26) (a) Tomasi, J.; Cammi, R.; Mennucci, B.; Cappelli, C.; Corni, S. *Phys. Chem. Chem. Phys.* **2002**, *4*, 5697−5712. (b) Cossi, M.; Scalmani, G.; Rega, N.; Barone, V. *J. Chem. Phys.* **2002**, *117*, 43−54.
(27) Tureček, F. *J. Phys. Chem. A* **1998**, *102*, 4703−4713.
(28) Chou, Y. C.; Liang, N. T.; Tse, W. S. *J. Raman Spectrosc.* **1986**, *17*, 481−484.

correspond to $CV^+$ ions that were deposited from the gas phase and adhered to the plasma-treated silver surface.

A possibility for deposition of neutral molecules transmitted from electrospray was also considered, as suggested by a reviewer. The most favorable scenario for neutral flux through the vacuum system can be represented by a viscous flow into the first vacuum chamber and an effusive flow through an orifice into the second vacuum chamber. It should be noted, however, that because of the relatively high pressure in the first chamber, the effusive flow approximation may exaggerate the flux through the second orifice by considering only the forward velocity component. According to an equation for effusive gas flow,[29] the flux density $f$ (in molecule $s^{-1}$ $cm^{-2}$) at distance $l$ from the orifice is given by (1), where $N_s$

$$f = \frac{1}{4} N_S \sqrt{\frac{8k_B T}{\pi m}} A_s \frac{1}{\pi l^2 \left(1 + \frac{r^2}{l^2}\right)^2} \quad (1)$$

is the molecule number density, $l$ is the target distance from the orifice, $r$ is the target off-axis distance, $A_s$ is the orifice area, $m$ is the mass of the molecule, $T$ is the absolute temperature, and $k_B$ is the Boltzmann constant. The flux (in molecule $s^{-1}$) through the orifice is given by eq 2. In our experiments, where $A_s = 0.031$

$$f_{orif} = N_S A_s \sqrt{\frac{8k_B T}{\pi m}} \quad (2)$$

$cm^2$ and $l = 10$ cm, the fraction of neutral molecules reaching the target at 10 cm is $f \times A_{target})/f_{orif} = 0.000\,156$. Note that the measured yield of $CV^+$,[7] which was deposited on a round spot of a 0.25-cm radius, was 0.1% or a 0.001 fraction of the total material that was electrosprayed. The ion transmission from the atmospheric pressure to the orifice was measured to be ~5%.[14a] Hence, in the absence of electrodynamic focusing, the fraction of gaseous crystal violet molecules arriving at the soft-landed spot is expected to be $0.000\,156 \times 0.05 = 7.8 \times 10^{-6}$ or 0.000 78% compared with the measured yield of 0.1%. Thus, about $100 \times 0.000\,78/0.1 =$ 0.8% of the detected and quantified soft-landed material could be due to penetrating neutrals. This analysis was further corroborated by experiments. First, in all experiments, the ion current that was monitored at the landing plate was proportional to the ion current from the electrospray needle. Neutral deposition could not generate a sustained current on the order of nanoamperes that we regularly observed on the target. Second, upon disconnecting one phase of the octopole ion guide, we observed a pronounced change in the shape of the spot of the deposited material from round to trapezoid (Figure S7, Supporting Information). The spot shape would not have changed had it been due to deposition of neutral species, because their trajectories could not be affected by the relatively weak multipolar field. Note that the crystal violet ion has no permanent dipole moment because of its $C_3$ symmetry. Third, when the landing plate was biased at +50 V to repel cations, no spot of crystal violet was formed after 3 h of exposure. Washing the plate yielded a barely detectable amount of crystal violet. However, the washed plate gave no SERS signal of $CV^+$. This proved beyond doubt that the material that was detected by SERS had arrived as cations from the gas phase.

The Raman active modes in both SERS and solution Raman spectra were assigned on the basis of a vibrational analysis using density functional theory calculations of $CV^+$ with the polarizable continuum model for aqueous solution (Figure 1b). The optimized structures of the ion are very similar in both the gas phase and aqueous solution and show a propeller-like geometry of $C_3$ symmetry (Figure 1b, inset). Both the solution Raman and SERS spectra of soft-landed $CV^+$ show some differences from the calculated spectrum. In particular, the peak of the out-of-phase ring stretch ($e_{41}$, 1609 $cm^{-1}$) is split into two peaks in the experimental Raman spectra that appear at 1588 and 1618 $cm^{-1}$ in the SERS spectrum of soft-landed $CV^+$ in Figure 1a. Similar splits occur in the reported SERS spectrum of adsorbed $CV^+$ (1620 and 1590 $cm^{-1}$)[28] and in the solution Raman spectrum (1622 and 1587 $cm^{-1}$, Figure S1, Supporting Information). However, the relative intensities of the two bands depend on the sample. With both the solution and adsorbed $CV^+$, the spectra show a major 1618−1622-$cm^{-1}$ component. With the soft-landed $CV^+$, the 1618- and 1588-$cm^{-1}$ band intensities are nearly equal. This indicates that this e mode, which involves a synchronous stretch of two of the three benzene rings in the $CV^+$ ion, is no longer degenerate in the surface-tethered ions. This may indicate that there are populations of species that adopt different orientations with respect to the surface that affect the vibrational frequency. The strong $CV^+$ band at 1363 $cm^{-1}$ in the solution Raman spectrum consists of the unresolved in-plane C−H bending mode ($e_{30}$) and symmetrical N−C-ring-C−C stretching mode ($e_{31}$) whose wavenumbers are calculated at 1352 and 1364 $cm^{-1}$, respectively. This band is notably broader in the SERS spectra of both adsorbed[28] and soft-landed $CV^+$, where it appears at 1368 and 1387 $cm^{-1}$ (Figure 1a). In contrast, the in-plane aromatic C−H bending modes ($e_{26}$ at 1186 $cm^{-1}$ and $e_{27}$ at 1193 $cm^{-1}$, Figure 1b) appear as a single enhanced band in the SERS spectrum at 1178 $cm^{-1}$ (Figure 1a). Substantial intensity enhancement is also found for the ring-breathing mode ($e_{18}$, calculated at 911 $cm^{-1}$), out-of-plane C−H bend ($e_{16}$, calculated at 796 $cm^{-1}$), and C−N−C symmetric stretch of the dimethylamino groups ($e_{14}$, calculated at 722 $cm^{-1}$), which appear at 914, 805, and 730 $cm^{-1}$, respectively, in the SERS spectrum (Figure 1a). The overall similarity of the SERS spectra of the soft-landed $CV^+$ with the reference $CV^+$ Raman spectra of ions that did not undergo hyperthermal collisions indicates that the surface-tethered ions retain the $CV^+$ bond connectivity and thus have not been damaged by hyperthermal impact on the surface.

**SERS Detection Limits.** We were interested in determining the lowest amount of immobilized $CV^+$ that can be detected on plasma-treated Ag substrate. This was tested by experiments where $CV^+$ was sprayed in mixtures with Rhodamine B as an internal standard and soft landed at 50 eV. The $CV^+$/Rhodamine B molar ratios were varied from 1:1 to 1:1000 in order to decrease the $CV^+$ loading while maintaining the total amount of the deposited material. We note that $CV^+$ and Rhodamine B have very similar ionization efficiencies in electrospray,[14a] and thus, the relative flux of soft-landed species is close to their relative concentrations in solution. In all these measurements, the loosely

(29) Anderson, J. B. Molecular Beams from Nozzle Sources, In *Molecular Beams and Low Density Gas Dynamics*; Wegener, P. P., Ed.; Marcel Dekker: New York, 1974; pp 16−21.

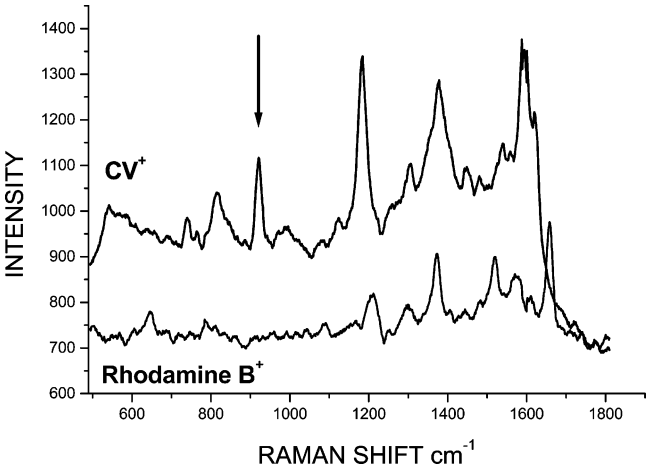


**Figure 2.** SERS spectra of soft-landed $CV^+$ (top trace) and Rhodamine B (bottom) that were deposited at comparable concentrations. The arrow indicates the unique peak at 914 $cm^{-1}$ that was used for $CV^+$ quantitation.

deposited ions were thoroughly washed off with solvent, so that only the surface-tethered ions were analyzed. Both $CV^+$ and Rhodamine B dyes produced intense SERS spectra (Figure 2) that were distinguished by the $e_{18}$ band at 914 $cm^{-1}$ that is unique for $CV^+$. The detection limit at 3 standard deviations of background was found at a 1:600 $CV^+$/Rhodamine B ratio. We consider the Raman active molecules to be in a monolayer that is in a close contact with the silver oxide surface, because the SERS effect fades away rapidly with distance from the surface.[17b] Taking into account the 0.8-$\mu m^2$ size of the spot that was irradiated by the excitation laser, and assuming close packing of the surface-bound ions of an 85-Å$^2$ cross section, we calculated the limit of detection for $CV^+$ at 2.5 zmol. Note that the total amount of the soft-landed material ($\sim 10^{-10}$ mol) was substantially greater than the measured detection limit. However, the low detection limits of the immobilized species are significant, because they allow us to characterize the species that modify the surface topical properties. The monolayer assumption was further tested by XPS analysis of soft-landed pure $CV^+$ in a sample that was thoroughly washed with methanol and furnished an intense SERS spectrum, such as the one shown in Figure 1a. However, in spite of the 5 atom % content of N in $CV^+$, which should be readily detectable in a surface monolayer, XPS was unable to detect the nitrogen 1s lines. This indicated that the surface coverage by the immobilized $CV^+$ was submonolayer. Hence, the above-estimated detection limits represent an upper bound for SERS of soft-landed ions.

From the comparison of the amount of $CV^+$ ions that provided the Raman signal from the 4 mM solution (>50 fmol) and the estimated amount of surface-bound $CV^+$ ions that gave rise to the SERS spectrum in Figure 1a (<600 zmol), we estimate the surface enhancement factor to be on the order of $10^5-10^6$, which is compatible with the enhancement factors predicted by the electromagnetic theory of SERS.[30]

A significant advantage of SERS spectroscopy of soft-landed ions is that the metal surface efficiently quenches analyte fluorescence. The SERS spectrum measured with a thick layer of ~0.5 nmol of soft-landed Rhodamine B that was not washed shows

(30) Moskovits, M. *J. Raman Spectrosc.* **2005**, *36*, 485−496.

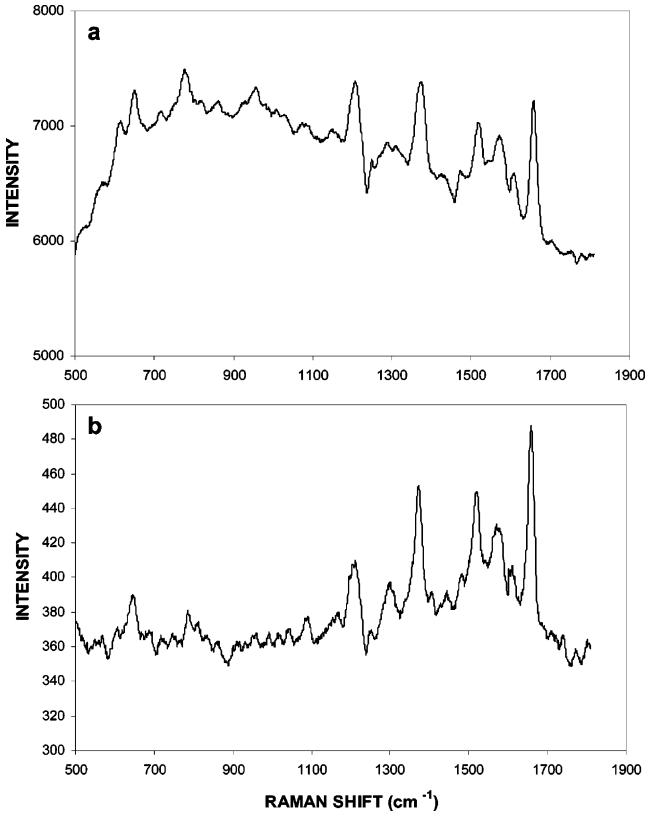


**Figure 3.** (a) SERS spectrum of Rhodamine B that was soft-landed on the plasma-treated Ag surface without washing. (b) SERS spectrum after washing off the unbound Rhodamine B. Note the >200-fold decrease of the fluorescence background centered around 537 nm.

an intense fluorescence band at 537 nm that obscures the Raman bands (Figure 3a). The fluorescence band completely disappears in the sample where the unbound layer of Rhodamine B was washed off leaving only the surface-bound material that shows an intense SERS spectrum (Figure 3b). This phenomenon is understandable given the known strong quenching effect of conductance band electrons in bulk metal[31] that decreases with the third power of distance from the surface[32] and thus mainly affects the surface-tethered species.

**Surface Properties.** The finding that the surface-immobilized material shows the essential features of the same species in solution raises the question of the nature of the surface and the analyte binding to it. To address this question, we first investigated the surface of the silver targets before and after treatment with air−Ar plasma and following soft landing. AFM scans of these silver targets revealed substantial differences. The untreated Ag surface shows a relatively low roughness (Figure 4a). The plasma-treated SERS-active surfaces show a number of ellipsoid-shaped protrusions that increase the average surface roughness to 22−24 nm, when expressed as an arithmetic average of deviations along the *z*-axis from the center plane (Figure 4b and c). The size of the protrusions in the $x-y$ plane is estimated from the AFM scans to be 20−40 nm, which is in the same range as for SERS-active metal colloid particles.[22] However, the important practical

(31) Waldeck, D. H.; Alivisatos, A. P.; Harris, C. B. *Surf. Sci.* **1985**, *158*, 103−125.
(32) Li, L.; Ruzgas, T.; Gaigalas, A. *Langmuir* **1999**, *15*, 6358−6363.

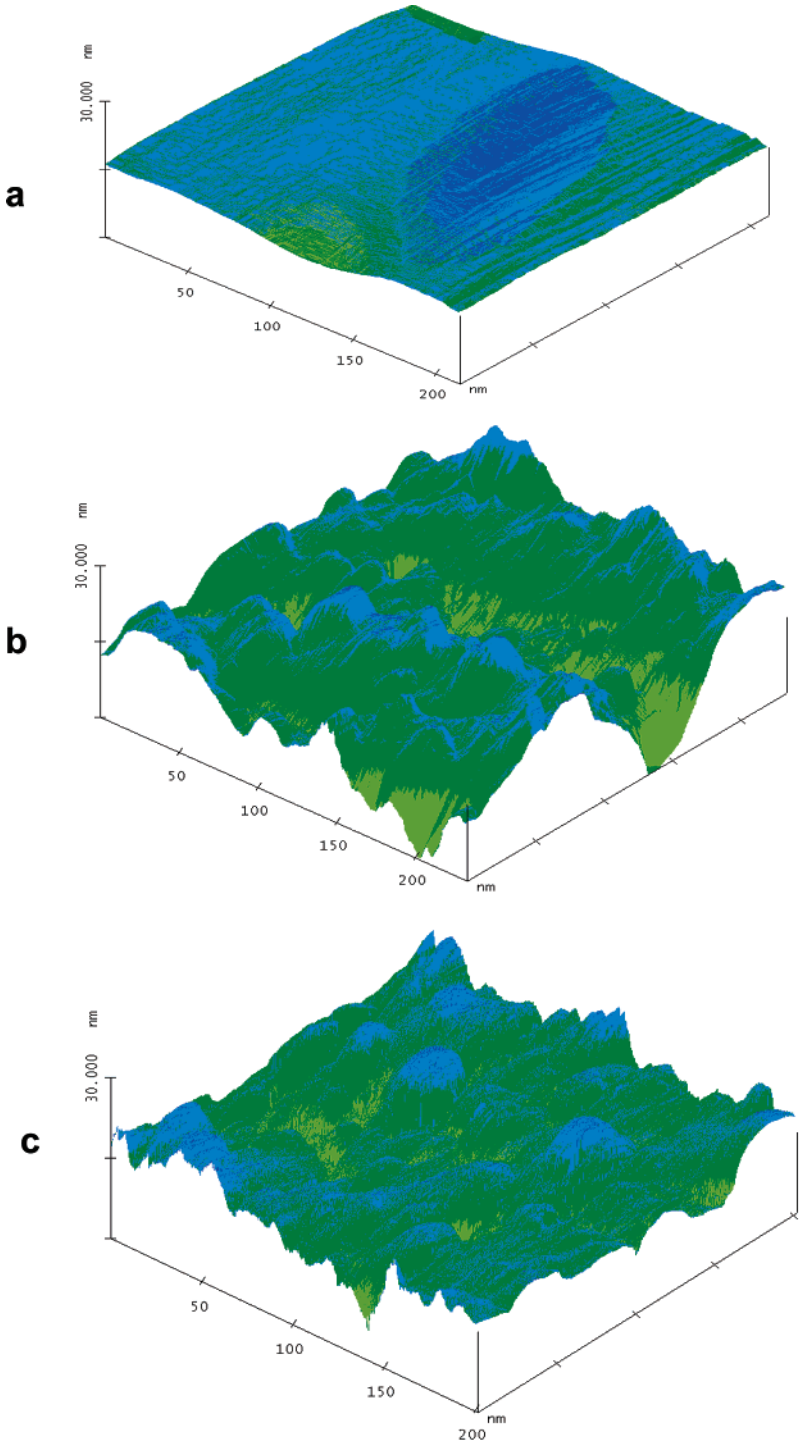


**Figure 4.** Atomic force microscopy scans of 200 × 200 nm sections of silver substrates. (a) Untreated Ag substrate, (b) plasma-treated Ag substrate, and (c) plasma-treated Ag with soft-landed $CV^+$ ions. The size of an $CV^+$ ion is much smaller as approximated by its van der Waals molecular radius (0.85 nm).

difference from colloidal Ag is that plasma-etched Ag surfaces can be made reproducibly SERS active, and they remain stable and SERS active for the period of several weeks, even when exposed to the atmosphere.

Surface oxidation is a necessary condition for nondestructive soft landing and immobilization of ions on metal surfaces.[8,14] SERS activity was shown previously for silver oxide layers sputtered on Al/glass substrates and exposed to photolytic reduction,[21b] and for silver atoms and ions sputtered on various metal and refractory substrates.[21a] In contrast to plasma treatment, the previous modes of activation for SERS relied on a photolytic modification of the surface by laser irradiation.[21] For plasma-treated Ag surfaces, the layer of silver oxide is reduced at the ion impact site by electrons from the bulk metal that are attracted by the positive charge of the soft-landed ion. The surface-tethered permanent cations such as $CV^+$ and Rhodamine B probably bind by ion pairing with oxide anions in the surface lattice. This is consistent with the SERS spectra of the soft-landed ions that show all features of Raman

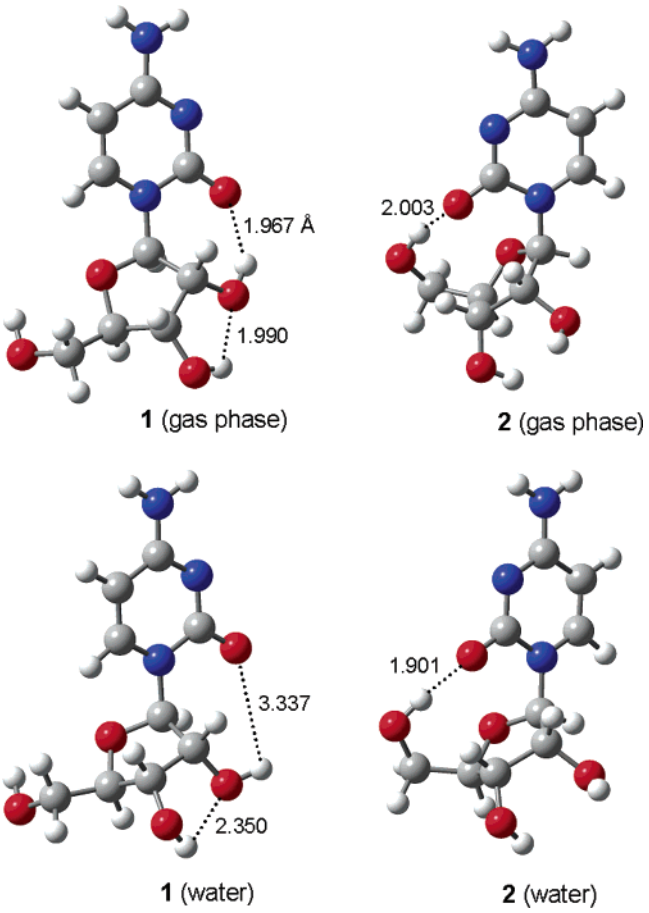


**Figure 5.** B3LYP/6-31+G(d,p) optimized structures of cytidine conformers **1** and **2** in the gas phase (top) and in the water dielectric (bottom). Broken lines indicate intramolecular hydrogen bonds in angstroms.

spectra of the corresponding ions in solution. Charge neutralization in the outer, loosely bound, layers of $CV^+$ probably occurs by ion pairing with hydrated $OH^-$ ions produced by reduction of the surface silver oxide layer. This mechanism is corroborated by an experiment in which an Ag substrate was plasma-treated in $O_2$ (0.3 Torr, 1.5 min, 60 W) to form a layer of silver oxides. This surface was dull black, nonconductive, and showed a morphology different from that of an untreated Ag surface when examined by optical microscopy. The treated surface was then exposed to the $CV^+$ ion beam at 50 eV and 2 nA. The substrate area that was exposed to the ion beam was found to be conductive and showed the formation of silver metal clusters that were visible by optical microscopy. In contrast, the surface area that was not exposed to the ion beam showed no changes. This indicates that the surface oxide layer undergoes reduction to generate counterions that compensate the coulomb charge of the soft-landed cations.

**Soft Landing of Nucleoside Ions.** The $CV^+$ and Rhodamine B dyes are rugged aromatic molecules that have absorption maxima near the 514.5-nm excitation wavelength from the Ar ion laser. Soft landing of such ions may be expected to yield undamaged material on the surface.[11,14] In addition, the SERS signal produced by surface-tethered $CV^+$ and Rhodamine B is amplified by resonant excitation of their chromophores. To explore the applicability of SERS for the characterization of more fragile biological molecules that lack chromophores for resonant excitation, we investigated soft landing of the DNA nucleobase cytosine and of the nucleosides cytidine and 2′-deoxycytidine. All these molecules produced singly protonated cations in electrospray that were soft landed on plasma-treated Ag substrates that were at a −40 V potential. The soft-landed samples of cytosine, cytidine, and 2′-deoxycytidine gave reproducible SERS spectra. The spectra were interpreted by comparing them with the experimental and calculated Raman spectra of the relevant cations and neutral molecules, as illustrated and discussed for cytidine.

In contrast to $CV^+$, which is a permanent ion, cytidine is protonated during electrospray and so the actual structures of the gas-phase ion(s) are of concern. We first address the structures and relative free energies of the species involved in the soft-landing experiments. Cytidine is calculated to form two stable conformers (**1** and **2**, Figure 5) that differ by the orientation of the nucleobase moiety with respect to the ribofuranose ring. Conformer **1**, in which the cytosine carbonyl is intramolecularly hydrogen bonded to $O_{(2')}$−H, is calculated to be 11 kJ $mol^{-1}$ more stable in the gas phase ($\Delta G_{g,298}$ value) than **2** in which the carbonyl is hydrogen bonded to $O_{(5')}$−H. The structures of cytidine conformers are affected by solvation with water. In particular, solvation of **1** disrupts the intramolecular hydrogen bond of the cytosine carbonyl (Figure 5) which affects the relative thermodynamic stabilities of solvated **1** and **2** that show $\Delta G_{aq,298}$ (**1** → **2**) = −0.3 kJ $mol^{-1}$. Gas-phase protonation of **1** is calculated to occur in the cytosine ring at $N_{(3)}$ producing ions **1**Ha$^+$ and **1**Hb$^+$ or at $O_{(2)}$ to produce **1**Hc$^+$. The corresponding gas-phase basicities were calculated as GB = 909, 924, and 903 kJ $mol^{-1}$, for the formation of **1**Ha$^+$, **1**Hb$^+$, and **1**Hc$^+$, respectively. Protonation at N-3 in **2** results in a disruption of the hydrogen bond to $O_{(5')}$−H, and the cytosine ring rotates to achieve structures **1**Ha$^+$ and **1**Hb$^+$ as local energy minima (Figure 6). Solvation in water prefers **1**Ha$^+$ over **1**Hb$^+$ and **1**Hc$^+$, as illustrated by the calculated $\Delta G_{rxn,298}$ for proton transfer to water (eqs 3−5).

$$\mathbf{1}\mathrm{Ha}^+(\mathrm{aq}) + \mathrm{H_2O}(\mathrm{aq}) \rightarrow \mathbf{1}(\mathrm{aq}) + \mathrm{H_3O}^+(\mathrm{aq}) \qquad \Delta G_{rxn,298} = 67\ \mathrm{kJ\ mol^{-1}} \quad (3)$$

$$\mathbf{1}\mathrm{Hb}^+(\mathrm{aq}) + \mathrm{H_2O}(\mathrm{aq}) \rightarrow \mathbf{1}(\mathrm{aq}) + \mathrm{H_3O}^+(\mathrm{aq}) \qquad \Delta G_{rxn,298} = 57\ \mathrm{kJ\ mol^{-1}} \quad (4)$$

$$\mathbf{1}\mathrm{Hc}^+(\mathrm{aq}) + \mathrm{H_2O}(\mathrm{aq}) \rightarrow \mathbf{1}(\mathrm{aq}) + \mathrm{H_3O}^+(\mathrm{aq}) \qquad \Delta G_{rxn,298} = 36\ \mathrm{kJ\ mol^{-1}} \quad (5)$$

Hence, the thermodynamic data indicate that cytidine ions formed by electrospray are likely to have structure **1**Ha$^+$.

The SERS spectrum of soft-landed **1**Ha$^+$ (Figure 7a) shows several bands that can be assigned on the basis of the Raman spectra that were measured in aqueous solution (Figure 7b) and also by comparison with the previous solution Raman and SERS spectra obtained on silver colloid particles.[33] Reference Raman spectra were also calculated for cytidine molecules in aqueous solution (Figure 7c) and for the cations in both gas-phase and aqueous solution (Figure S9, Supporting Information).

(33) Sánches-Cortés, S.; Molina, M.; García-Ramos, J. V.; Carmona, P. *J. Raman Spectrosc.* **1991**, *22*, 819−824.

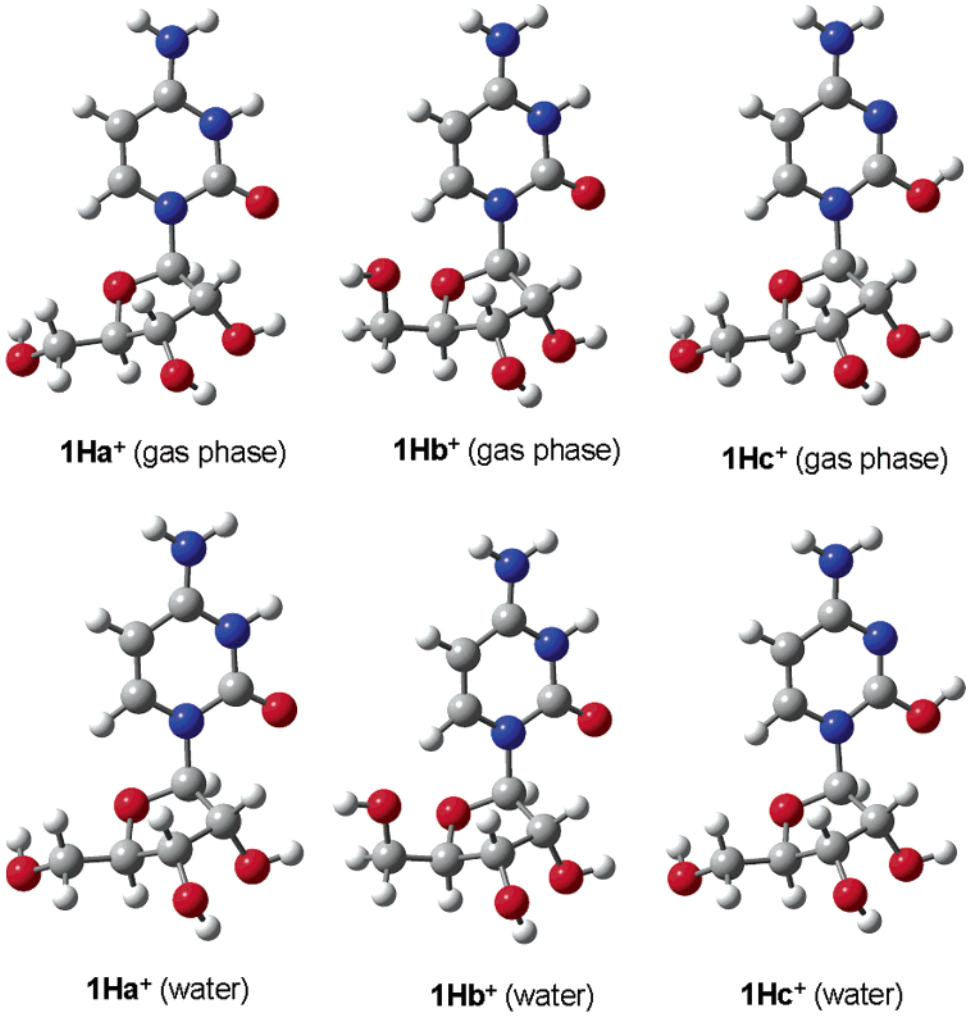


**Figure 6.** B3LYP/6-31+G(d,p) optimized structures of conformers of N-3 protonated cytidine cation **1**Ha$^+$ and **1**Hb$^+$ and the O-2 protonated tautomer **1**Hc$^+$. Top structures show gas-phase ions; bottom structures are for cations in the water dielectric.

The Raman spectrum of aqueous cytidine (Figure 7b) matches well the spectrum calculated for conformer **1** and shows four main groups of bands at 794, 1225−1302, 1537, and 1604−1618 cm$^{-1}$. We note that the Raman spectra are sensitive to the nucleobase conformation, as conformer **2** gives a very different band pattern (Figure S8, Supporting Information).

In comparison with the reference spectra, the SERS spectrum in Figure 7a shows substantially broadened bands in most of the wavelength region. An exception is the SERS-enhanced band at 795 cm$^{-1}$ corresponding to the cytosine ring deformation mode of the $N_{(1)}-C_{(2)}-N_{(3)}$ bonds, which matches the 794-cm$^{-1}$ band in the reference spectrum (Figure 7b). The band centered at 987 cm$^{-1}$, which is also enhanced and broadened, corresponds to a cytosine ring combined in-plane C−H and N−H deformation mode that appears at 1003 cm$^{-1}$ in the reference spectrum. The C−H in-plane deformation mode (1225 cm$^{-1}$) and the ribose $C_{(1')}-H_{(1')}$ and $C_{(2')}-H_{(2')}$ out-of-plane mode (1253 cm$^{-1}$) also appear in the SERS spectrum. However, they overlap with the intense bands between 1321 and 1358 cm$^{-1}$ that are weak in the solution spectrum where they correspond to several combined deformation modes of the ribose C−H bonds. The cytosine ring stretching modes at 1537, 1604, and 1618 cm$^{-1}$ are rather poorly resolved in the SERS spectrum of soft-landed cytidine. We note that the strong Raman band of the asymmetric $C_{(5)}-C_{(4)}-N_{(3)}$ ring stretch (calculated at 1547 cm$^{-1}$, measured at 1528 cm$^{-1}$)[33] is relatively less enhanced in SERS for both soft-landed ions and cytidine absorbed on silver colloids.[33] Also noteworthy is the shoulder at 1637 cm$^{-1}$ in the SERS spectrum that corresponds to the symmetric $C_{(5)}-C_{(6)}$ and $C_{(2)}-N_{(3)}$ combination stretch in the cytosine ring of the solvated molecule at 1636 cm$^{-1}$ (Figure 7b). We note that this band was previously assigned to the C=O stretch,[33,34] but the present vibrational analysis clearly identifies it as the above-mentioned combination mode. In contrast, the C=O stretch in gas-phase cytidine, which is calculated to be at 1690 cm$^{-1}$, is very weak in the SERS spectrum, which indicates that the surface-bound molecules are mostly microsolvated. The SERS spectrum also differs in several wavenumbers from the calculated Raman spectra of rotamers of protonated cytidine cations (Figure S9, Supporting Information). This indicates that the molecules on the surface are neutral, and hence, the soft-landed cations must have been neutralized by proton transfer to the oxide layer.[8,11]

The substantial broadening of the active bands in the SERS spectrum can be interpreted by multiple conformations of the cytidine molecules that are likely to be deposited at random orientations on the surface. Regarding conformation effects, cytidine conformer **2** is calculated to have Raman bands at 1372

(34) Lord, R. C.; Thomas, Jr., G. J. *Spectrochim. Acta, Part A* **1967**, *23A*, 2551−2568.

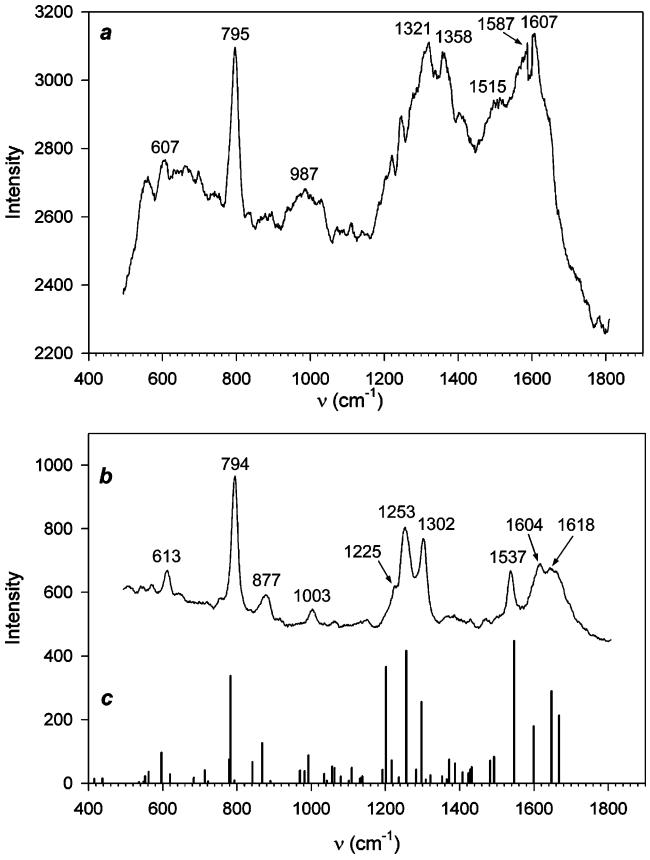


**Figure 7.** (a) SERS spectrum of cytidine soft-landed at 40 eV on a plasma-treated silver substrate. (b) Reference Raman spectrum of cytidine measured in aqueous solution, (c) PCM-B3LYP/6-31+G(d,p) calculated Raman spectrum of cytidine conformer **1** in the water dielectric. The wavenumbers in the calculated spectrum were scaled by 0.981.

and 1514 $cm^{-1}$ (Figure S8, Supporting Information), which, if enhanced by SERS, could give rise to the observed bands near 1358 and 1515 $cm^{-1}$. Multiple orientations on the surface can also explain the substantial peak broadening in the SERS spectra, because both the intensity and wavenumbers of the Raman bands depend on the contact with the Ag surface. Despite the band broadening, the match between several Raman-active modes in soft-landed molecules and those in solution indicates that a fraction of the soft-landed molecules were not damaged by the 40−50-eV impact with the surface, nor did they form covalent bonds to the oxide layer that would disrupt the weak $N_{(1)}-C_{(1')}$ cytosine−sugar glycosidic bond to affect the Raman spectrum.

The nature of bonding to the surface can be deduced only indirectly from the present data. The SERS spectra indicate that the soft-landed molecules do not develop covalent bonds to the surface atomic or molecular species as previously thought.[7] It appears likely that the bonding is mediated by $\pi$-coordination of the cytosine ring to the surface silver atoms and ions.

In summary, polyatomic cations that are soft-landed on plasma-treated Ag surfaces at hyperthermal impact energies exhibit reproducible surface-enhanced Raman scattering effects that can be used to characterize the chemical nature of the surface-bound ions and molecules. From the present study, it appears that the molecules are bound to the surface by $\pi$-coordination to the Ag atoms and ions. The finding that reproducible SERS soft-landed polyatomic ions can be routinely obtained opens new avenues to investigate soft-landing technology for the fabrication of bioactive metal surfaces and biomolecule immobilization.

## ACKNOWLEDGMENT

Financial support by the University of Washington Royalty Research Fund, the National Science Foundation (Grants CHE-0349595, CHE-0342956, and ATM-0323930), and the Leonard X. Bosack and Bette M. Kruger Charitable Foundation is gratefully appreciated. M.V. thanks the Gudiksen Fellowship for support. Thanks are also due to Matt S. Diener and Karl E. Jackson for technical assistance with SERS measurements.

## SUPPORTING INFORMATION AVAILABLE

Complete ref 24; Tables S1 and S2 of calculated energies and active Raman band intensities and assignments; Figures S1−S9 with experimental and calculated Raman spectra. This information is available free of charge via the Internet at www.pubs.acs.org.

Received for review February 9, 2007. Accepted April 13, 2007.

AC070278A